

Diastereoselective Routes to [Amino($\sigma(P):\eta^6$ -(ansa-phosphinite)benzene)chlororuthenium(II)] PF₆ Salts: Kinetic versus Thermodynamic Preferences

Immo Weber,^{†,‡} Frank W. Heinemann,[†] Walter Bauer,[±] Stefano Superchi,[‡] Achim Zahl,[†] Daniela Richter,^{||} and Ulrich Zenneck^{*,†}

Department Chemie und Pharmazie, Erlangen Catalysis Resource Center (ECRC), and Interdisciplinary Center for Molecular Materials (ICMM), Friedrich-Alexander-Universität Erlangen-Nürnberg, Egerlandstrasse 1, D-91058 Erlangen, and Henkestrasse 42, D-91054 Erlangen, Germany, Dipartimento di Chimica, Università della Basilicata, via Nazario Sauro 85, I-85100 Potenza, Italy, and Computer Chemistry Center and ICMM, Friedrich-Alexander-Universität Erlangen-Nürnberg, Nögelsbachstrasse 25, D-91052 Erlangen, Germany

Received December 17, 2007

A novel chiral phosphinite derivative was designed as a ligand for Ru²⁺ ions to give access to new enantiomerically pure or diastereomerically enriched [$\sigma(P):\eta^6$ -(ansa-phosphinite)benzene]Ru(II) complexes. We are interested in this class of compounds as potential catalysts for enantioselective transfer hydrogenation of organic carbonyl compounds. The preparation of enantiopure (*R*)-[$\sigma(P):\eta^6$ -(ansa-phosphinite)benzene]Ru(II)Cl₂ (**6**) was achieved in good yield on the basis of (*S*)-mandelic acid. Four diastereomeric [$\sigma(P):\eta^6$ -(ansa-phosphinite)benzene]Ru(II)Cl(NH₂R)]⁺ complex PF₆⁻ salts were obtained from neutral **6** by nucleophilic substitution of a chloride ligand with primary amines. For aniline and *p*-fluoroaniline salts **7** and **8** a significant excess of the (*S*_{Ru},*R*_C)-diastereomers **7S** and **8S** was observed in the reaction mixtures as the kinetically preferred species, and **7S** could be isolated as a pure diastereomer. No diastereoselectivity was observed in the reaction mixtures of (*R*)- and (*S*)-1-phenylethylamine salts **9** and **10** right after preparation. **7**, **8**, and **9** epimerize at the metal center. This leads to a loss of diastereoselectivity of **7S** and **8S** but enrichment of (*R*_{Ru},*R*_C)-diastereomer **9R**. Pure diastereomers **7S**, **9R**, and **10S** as well as a 1:1 diastereomeric mixture **8S/8R** have been characterized structurally. The experimental setup allowed detailed insight into the specific X-ray crystallographic, CD, and NMR spectroscopic properties of defined stereoisomers of chiral Ru(II) complexes. The kinetic diastereoselectivities of **7S** and **8S** are explained by a H-bond delivery effect, while pure diastereomer salt **9R** is configuratively stable.

Introduction

Configurationally stable *hapto*-arene complexes with pseudo-tetrahedral chiral metal centers¹ and especially chiral Ru(II) η^6 -arene complexes have gained increasing interest after their discovery by Noyori as enantioselective catalysts for transfer hydrogenations.² In the scope of potential enantioselective catalysts an *ansa* linkage from the η^6 -arene ligand of such complexes via an alkyl chain with a terminal σ -donor functionality complexed to the pseudotetrahedral Ru(II) center bears unique structural features: (i) An *ansa* chain with two to three

atoms as covalent links besides the σ -donor functionality stabilizes the η^6 -arene moiety toward substitution. (ii) A chiral *ansa* chain can serve as a provider of “chiral information” in the sense that it closes up one diastereotopic side of the Ru(II) center and creates a “chiral pocket” around it.

Thus, not only could ligand substitution proceed diastereoselectively, but also the resulting chiral Ru(II) center should be

* To whom correspondence should be addressed. E-mail: ulrich.zenneck@chemie.uni-erlangen.de. Tel: int +49 9131 8527464. Fax: int +49 9131 8527367.

[†] Anorganische Chemie, FAU Erlangen-Nürnberg.

[±] Organische Chemie, FAU Erlangen-Nürnberg.

[‡] Università della Basilicata.

^{||} Computer Chemistry Center FAU Erlangen-Nürnberg.

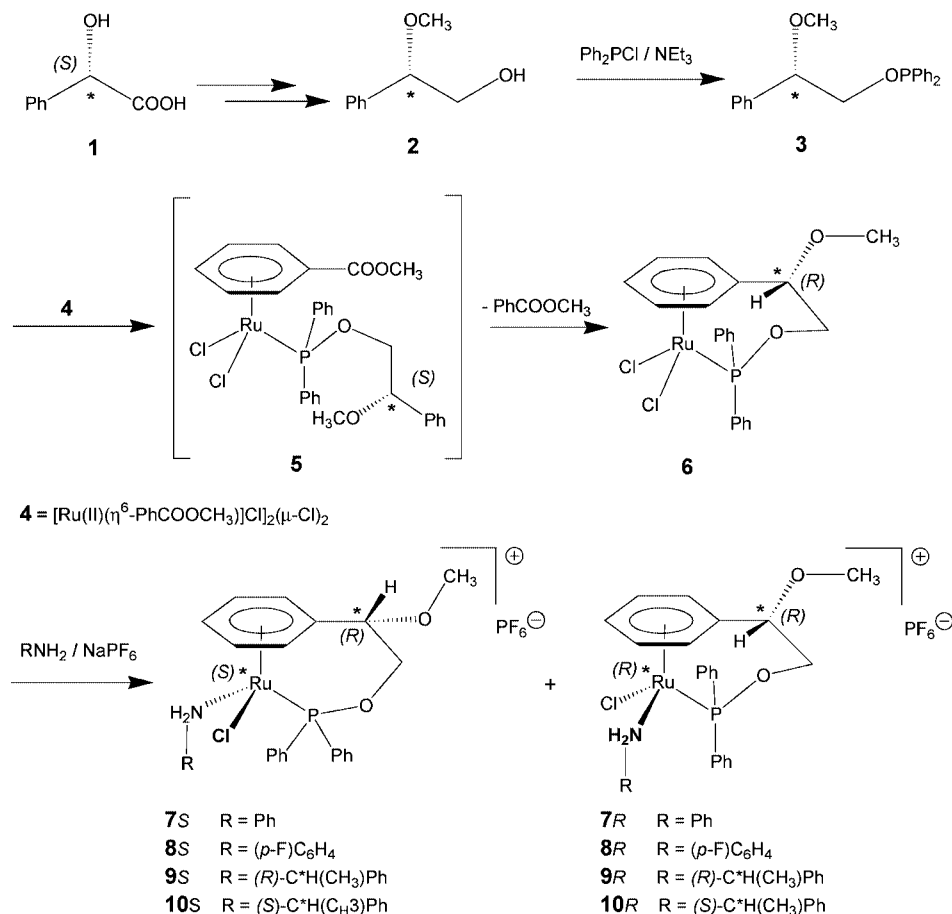
[‡] Present address: Institut für Physikalische Chemie, Technische Universität Bergakademie Freiberg, Leipziger Str. 29, D-09596 Freiberg, Germany.

(1) (a) Brunner, H.; Gasting, R. G. *J. Organomet. Chem.* **1978**, *145*, 365. (b) Brunner, H.; Nuber, B.; Pommersberger, M. *Tetrahedron: Asymmetry* **1998**, *9*, 3223. (c) Brunner, H. *Enantiomer* **1997**, *2*, 133. (d) Brunner, H. *Angew. Chem., Int. Ed.* **1999**, *38*, 1194. (e) Brunner, H. *Eur. J. Inorg. Chem.* **2001**, 905. (f) Pertici, P.; Pitzalis, E.; Marchetti, F.; Rosini, C.; Salvatori, P. *J. Organomet. Chem.* **1994**, *466*, 221. (g) Davenport, A. J.; Davies, D. L.; Fawcett, J.; Russel, D. R. *J. Chem. Soc., Perkin Trans. 1* **2001**, 1500.

(2) (a) Blaser, H.-U.; Malan, C.; Pugin, B.; Spindler, F.; Steiner, H.; Studer, M. *Adv. Synth. Catal.* **2003**, *345*, 103, and references therein. (b) Noyori, R.; Ohkuma, T. *Angew. Chem., Int. Ed.* **2001**, *40*, 40, and references therein. (c) Hashiguchi, S.; Fujii, A.; Takehara, J.; T.; Ikariya, T.; Noyori, R. *J. Am. Chem. Soc.* **1995**, *117*, 7562. (d) Haack, K.-J.; Hashiguchi, S.; Fujii, A.; Ikariya, T.; Noyori, R. *Angew. Chem., Int. Ed. Engl.* **1997**, *36*, 285. (e) Haack, K.-J.; Hashiguchi, S.; Fujii, A.; Ikariya, T.; Noyori, R. *Angew. Chem., Int. Ed. Engl.* **1997**, *36*, 288. (f) Yamakawa, M.; Yamada, I.; Noyori, R. *Angew. Chem., Int. Ed.* **2001**, *40*, 2818. (g) Yamakawa, M.; Ito, H.; Noyori, R. *J. Am. Chem. Soc.* **2000**, *122*, 1466. (h) Fujii, A.; Hashiguchi, S.; Uematsu, N.; Ikariya, T.; Noyori, R. *J. Am. Chem. Soc.* **1996**, *118*, 2521. (i) Palmer, M. J.; Wills, M. *Tetrahedron: Asymmetry* **1999**, *10*, 2045, and references therein. (j) Sortuis, J.-B.; Ritleng, V.; Voelklin, A.; Moluige, A.; Smail, H.; Barloy, L.; Sirlin, C.; Verzijl, G. K. M.; Boogers, J. A. F.; de Vries, A. H. M.; de Vries, J. G.; Pfeffer, M. *Org. Lett.* **2005**, *7*, 1247.

(3) (a) Miyaki, Y.; Onishi, T.; Kurosawa, H. *Inorg. Chim. Acta* **2000**, *300–302*, 369. (b) Marconi, G.; Baier, H.; Heinemann, F. W.; Pinto, P.; Pritzkow, H.; Zenneck, U. *Inorg. Chim. Acta* **2003**, *352*, 188. (c) Bodes, G.; Heinemann, F. W.; Marconi, G.; Neumann, S.; Zenneck, U. *J. Organomet. Chem.* **2002**, *641*, 90. (d) Bodes, G.; Heinemann, F. W.; Jobi, G.; Klodwig, J.; Neumann, S.; Zenneck, U. *Eur. J. Inorg. Chem.* **2003**, 281.

Scheme 1. Syntheses of Diastereomeric Complex Salts $\{[\eta^6:\sigma(P)$ -(arene-ansa-phosphinite)]Ru(II)(amino)(chloro) $\}^+\text{PF}_6^-$ 7–10 Starting from Natural (*S*)-Mandelic Acid (1)



influenced in its configurational stability via diastereomeric interaction with the chiral *ansa* chain. Within this scope Ru(II) η^6 -arene complexes containing nitrogen and oxygen^{3a,b} as well as phosphorus and carbene⁴ donor groups at the terminus of the *ansa* chain attracted attention. In previous studies we also investigated a series of Ru(0) η^6 -arene complexes containing unlinked chiral chains with N- and O-donors.^{3c,d} Ward succeeded in the full configurational stabilization of a chiral Ru(II) center by anchoring the metal in a rigid bicyclic *ansa* framework connected with a η^6 -arene ligand.^{5a} Pregosin achieved an unprecedented stabilization of a notorious labile η^6 -naphthalene ligand in a Ru(II) complex just by *ansa* linkage.^{5b} Willis reported a major breakthrough with this concept by stabilizing Noyori's (*S,S*)-TsDPEN Ru(II) catalyst via an *ansa* linkage to its η^6 -arene ligand, thus achieving unchanged high enantioselectivity

in the transfer hydrogenation of ketones with a higher TON.^{5c} This proved *ansa* linking and stabilized the catalyst in the sense of a “three-point-attachment”. Previously we reported on [$\sigma(P)$]: η^6 -(ansa-phosphine)benzene and [$\sigma(P)$]: η^6 -(ansa-phosphetane)benzene Ru(II)Cl $_2$ complexes^{5d,e} and studied diastereoselective nucleophilic substitutions of one chloride ligand by various amines resulting in cationic complexes with chiral Ru(II) centers. This simple two-step synthetic strategy enabled us to screen a large variety of *ansa*-linked Ru(II) η^6 -arene complexes as potentially enantioselective transfer hydrogenation catalysts

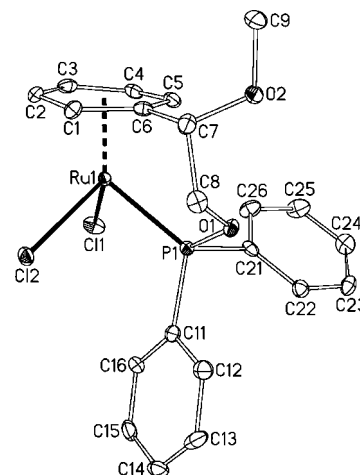


Figure 1. Thermal ellipsoid plot (50% probability) of the molecular structure of chiral complex 6: (*R*), methoxy group “out of plane”; hydrogen atoms omitted for clarity; selected bond distances and angles, see Table 1.

(4) (a) Jung, S.; Ilg, K.; Brandt, C. D.; Wolf, J.; Werner, H. *J. Chem. Soc., Dalton Trans.* **2002**, 318. (b) Smith, P. D.; Wright, A. J. *J. Organomet. Chem.* **1998**, 559, 141. (c) Simal, F.; Jan, D.; Demonceau, A.; Noels, A. F. *Tetrahedron Lett.* **1999**, 40, 1653. (d) Fürstner, A.; Liebl, C.; Lehmann, C. W.; Picquet, M.; Kunz, R.; Bruneau, C.; Touchard, D.; Dixneuf, P. H. *Chem.—Eur. J.* **2000**, 6, 1847. (e) Bennett, M. A.; Edwards, A. J.; Harper, J. R.; Kimyak, T.; Willis, A. C. *J. Organomet. Chem.* **2001**, 629, 7. (ee) Nelson, J. H.; Ghebreyessus, K. Y.; Cook, V. C.; Edwards, A. J.; Wielandt, W.; Wild, S. B.; Willis, A. C. *Organometallics* **2002**, 21, 1727. (f) Özdemir, I.; Demir, S.; Çetinkaya, B.; Toupet, L.; Castarlenas, R.; Fischmeister, C.; Dixneuf, P. H. *Eur. J. Inorg. Chem.* **2007**, 2862. (g) Faller, J. W.; Fontaine, P. P. *J. Organomet. Chem.* **2007**, 692, 976.

(5) (a) Therrien, B.; König, A.; Ward, T. R. *Organometallics* **2001**, 20, 2990. (b) Geldbach, T. J.; Pregosin, P. S.; Bassetti, M. *Organometallics* **2001**, 20, 2990. (c) Hannedouche, J.; Clarkson, G. J.; Willis, M. J. *Am. Chem. Soc.* **2004**, 126, 986. (d) Pinto, P.; Marconi, G.; Heinemann, F. W.; Zenneck, U. *Organometallics* **2004**, 23, 374. (e) Pinto, P.; Götz, A. W.; Hess, B. A.; Marinetti, A.; Heinemann, F. W.; Marconi, G.; Zenneck, U. *Organometallics* **2006**, 25, 2607.

Table 1. Selected Bond Distances and Angles of Chiral Complex 6

distance	[Å]	angle	[deg]
Ru(1)–Cl(1)	2.4080(8)	Cl(1)–Ru(1)–Cl(2)	86.51(3)
Ru(1)–Cl(2)	2.4089(7)	P(1)–Ru(1)–Cl(1)	89.20(3)
Ru(1)–P(1)	2.2927(8)	P(1)–Ru(1)–Cl(2)	90.90(3)
Ru(1)–C(1)	2.185(3)	P(1)–Ru(1)–C(1)	117.43(11)
Ru(1)–C(2)	2.288(3)	P(1)–Ru(1)–C(2)	154.87(8)
Ru(1)–C(3)	2.287(3)	P(1)–Ru(1)–C(3)	152.14(8)
Ru(1)–C(4)	2.184(3)	P(1)–Ru(1)–C(4)	114.51(9)
Ru(1)–C(5)	2.186(2)	P(1)–Ru(1)–C(5)	88.22(11)
Ru(1)–C(6)	2.214(3)	P(1)–Ru(1)–C(6)	89.72(8)
P(1)–O(1)	1.633(2)	C(9)–O(2)–C(7)	113.0(2)
C(8)–O(1)	1.446(4)	C(6)–C(7)–O(2)	111.5(3)
C(7)–C(8)	1.510(4)	C(6)–C(7)–C(8)	112.5(3)
C(6)–C(7)	1.518(4)	C(7)–C(8)–O(1)	110.4(2)
C(7)–O(2)	1.419(4)	C(8)–O(1)–P(1)	118.8(2)
C(9)–O(2)	1.427(4)	O(1)–P(1)–Ru(1)	111.03(8)

in a combinatorial-divergent approach. However, enantioselectivities achieved in the transfer hydrogenation of ketones with this class of diastereomeric complexes were surprisingly low despite their high configurational stability.^{5d} Therefore we searched for novel $\{\sigma(\text{Do}):\eta^6\text{-}(ansa\text{-benzene})\text{Ru(II)}\}$ complexes (Do = benzene side chain donor functionality), which influence the electronic situation of a transition metal center. Here we report on the approach to replace the *ansa*-phosphine by an *ansa*-phosphinite arene ligand based on cheap natural (*S*)-mandelic acid, **1**. Phosphinite Ru(II) complexes already proved to be successful in enantioselective hydrogenation and transfer

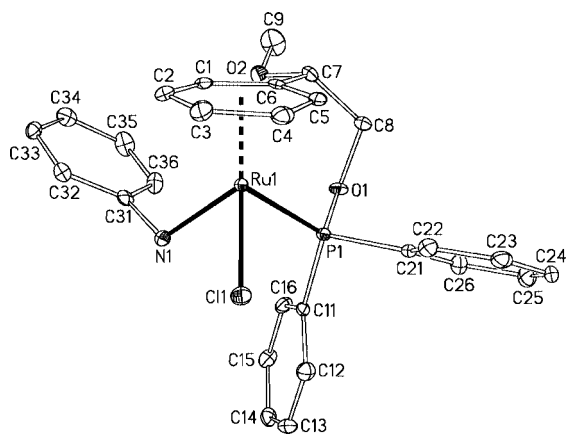


Figure 2. Thermal ellipsoid plot (50% probability) of the molecular structure of diastereomeric complex cation of PF_6^- salt **7S**: (S_{Ru} , R), methoxy group “in plane”; hydrogen atoms omitted for clarity; selected bond distances and angles, see Table 3.

Table 2. Selected Bond Distances and Angles of the Complex Cation of PF_6^- Salt 7S

distance	[Å]	angle	[deg]
Ru(1)–Cl(1)	2.3958(6)	Cl(1)–Ru(1)–P(1)	87.00(2)
Ru(1)–P(1)	2.2944(6)	Cl(1)–Ru(1)–N(1)	82.60(5)
Ru(1)–N(1)	2.182(2)	P(1)–Ru(1)–N(1)	90.72(5)
Ru(1)–C(1)	2.196(2)	P(1)–Ru(1)–C(2)	154.36(6)
Ru(1)–C(2)	2.286(2)	P(1)–Ru(1)–C(3)	152.77(6)
Ru(1)–C(3)	2.278(2)	N(1)–Ru(1)–C(4)	153.50(8)
Ru(1)–C(4)	2.192(2)	N(1)–Ru(1)–C(5)	157.46(7)
Ru(1)–C(5)	2.194(2)	Cl(1)–Ru(1)–C(1)	155.48(6)
Ru(1)–C(6)	2.195(2)	Cl(1)–Ru(1)–C(6)	157.73(6)
P(1)–O(1)	1.621(2)	C(9)–O(2)–C(7)	115.0(2)
C(8)–O(1)	1.447(3)	C(6)–C(7)–O(2)	106.8(2)
C(7)–C(8)	1.525(3)	C(6)–C(7)–C(8)	114.1(2)
C(6)–C(7)	1.524(3)	C(7)–C(8)–O(1)	113.2(2)
C(7)–O(2)	1.417(3)	C(8)–O(1)–P(1)	119.3(2)
C(9)–O(2)	1.419(3)	O(1)–P(1)–Ru(1)	111.97(6)
N(1)–C(31)	1.457(3)	Ru(1)–N(1)–C(31)	117.2(2)

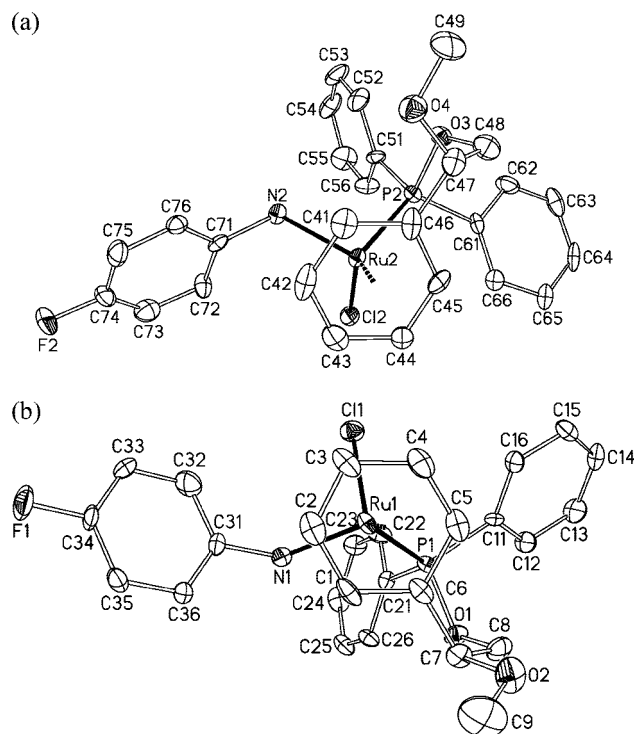


Figure 3. Thermal ellipsoid plot (50% probability) of the molecular structure of the diastereomeric complex cations of PF_6^- salt **8** taken out of a common unit cell (top views on the η^6 -arene moieties, hydrogen atoms omitted for clarity): (a) **8S** (S_{Ru} , R), methoxy group “in plane”; (b) **8R** (R_{Ru} , R), methoxy group “out of plane”; selected bond distances and angles, see Table 3 for **8S** and Table 4 for **8R**. Note the pseudomirror positions of the equatorial phosphinite phenyl groups and the *p*-fluoroaniline ligands in both diastereomers.

Table 3. Selected Bond Distances and Angles of the Complex Cation of PF_6^- Salt 8S

distance	[Å]	angle	[deg]
Ru(2)–Cl(2)	2.396(2)	Cl(2)–Ru(2)–P(2)	86.37(5)
Ru(2)–P(2)	2.287(2)	Cl(2)–Ru(2)–N(2)	83.2(2)
Ru(2)–N(2)	2.181(4)	P(2)–Ru(2)–N(2)	87.6(2)
Ru(2)–C(41)	2.219(6)	P(2)–Ru(2)–C(42)	149.7(2)
Ru(2)–C(42)	2.262(5)	P(2)–Ru(2)–C(43)	158.4(2)
Ru(2)–C(43)	2.235(6)	N(2)–Ru(2)–C(44)	150.4(2)
Ru(2)–C(44)	2.197(6)	N(2)–Ru(2)–C(45)	161.4(2)
Ru(2)–C(45)	2.212(5)	Cl(2)–Ru(2)–C(41)	160.8(2)
Ru(2)–C(46)	2.222(5)	Cl(2)–Ru(2)–C(46)	151.5(2)
P(2)–O(3)	1.624(4)	C(49)–O(4)–C(47)	114.8(4)
C(48)–O(3)	1.446(6)	C(46)–C(47)–O(4)	108.1(4)
C(47)–C(48)	1.534(6)	C(46)–C(47)–C(48)	113.5(4)
C(46)–C(47)	1.525(8)	C(47)–C(48)–O(3)	111.4(4)
C(47)–O(4)	1.415(5)	C(48)–O(3)–P(2)	117.2(3)
C(49)–O(4)	1.437(6)	O(3)–P(2)–Ru(2)	112.2(2)
N(2)–C(71)	1.468(7)	Ru(2)–N(2)–C(71)	117.9(3)
F(2)–C(74)	1.366(6)		

hydrogenation reactions of ketones,⁶ also, but to the best of our

(6) (a) Caballero, A.; Jalón, F. A.; Manzano, B. R.; Espino, G.; Pérez-Manrique, M.; Mucientes, A.; Poblete, F. J.; Maestro, M. *Organometallics* **2004**, *23*, 5694. (b) Tribó, R.; Muñoz, S.; Pons, J.; Yáñez, R.; Álvarez-Larena, Á.; Piniella, J. F.; Ros, J. *J. Organomet. Chem.* **2005**, *690*, 4072. (c) Blandin, V.; Carpentier, J.-F.; Mortreux, A. E. *J. Org. Chem.* **1999**, *1787*. (d) Guo, R.; Elpelt, C.; Chen, X.; Song, D.; Morris, R. H. *Chem. Commun.* **2005**, 3050. (e) Guo, R.; Chen, X.; Elpelt, C.; Song, D.; Morris, R. H. *Org. Lett.* **2005**, *7*, 1757. (f) Pasquier, C.; Naili, S.; Mortreux, A.; Agbossou, F.; Pélineski, L.; Brocard, J.; Eilers, J.; Reiners, I.; Peper, V.; Martens, J. *Organometallics* **2000**, *19*, 5723. (g) Cerón-Camacho, R.; Gómez-Benítez, V.; Le Lagadec, R.; Morales-Morales, D.; Toscano, R. *J. Mol. Catal. A* **2006**, *247*, 124.

Table 4. Selected Bond Distances and Angles of the Complex Cation of PF_6^- Salt **8R**

distance	[Å]	angle	[deg]
Ru(1)–Cl(1)	2.387(2)	Cl(1)–Ru(1)–P(1)	86.76(5)
Ru(1)–P(1)	2.294(2)	Cl(1)–Ru(1)–N(1)	82.9(2)
Ru(1)–N(1)	2.154(4)	P(1)–Ru(1)–N(1)	88.3(2)
Ru(1)–C(1)	2.176(5)	P(1)–Ru(1)–C(2)	153.5(2)
Ru(1)–C(2)	2.275(5)	P(1)–Ru(1)–C(3)	155.9(2)
Ru(1)–C(3)	2.302(5)	N(1)–Ru(1)–C(4)	152.9(2)
Ru(1)–C(4)	2.200(6)	N(1)–Ru(1)–C(5)	158.8(2)
Ru(1)–C(5)	2.201(6)	Cl(1)–Ru(1)–C(1)	156.5(2)
Ru(1)–C(6)	2.176(5)	Cl(1)–Ru(1)–C(6)	156.3(2)
P(1)–O(1)	1.622(4)	C(9)–O(2)–C(7)	114.2(4)
C(8)–O(1)	1.449(6)	C(6)–C(7)–O(2)	108.7(4)
C(7)–C(8)	1.528(6)	C(6)–C(7)–C(8)	115.9(4)
C(6)–C(7)	1.502(7)	C(7)–C(8)–O(1)	111.6(4)
C(7)–O(2)	1.409(5)	C(8)–O(1)–P(1)	119.7(3)
C(9)–O(2)	1.423(6)	O(1)–P(1)–Ru(1)	112.6(2)
N(1)–C(31)	1.455(7)	Ru(1)–N(1)–C(31)	116.2(3)
F(1)–C(34)	1.377(5)		

knowledge only Kurosawa reported $[\sigma(P):\eta^6\text{-}(ansa\text{-phosphinite})\text{benzene}]\text{Ru(II)Cl}_2$ complexes he obtained by coordination of chlorophosphines on a 3-hydroxypropyl Ru(II) η^6 -arene dimer followed by intramolecular alcoholysis.^{3a} We wish to present a chiral version of such Ru(II) η^6 -arene complexes with a chiral *ansa*-phosphinite chain that we complementary obtained by an η^6 -arene exchange reaction, previously attempted by Ward.^{5a}

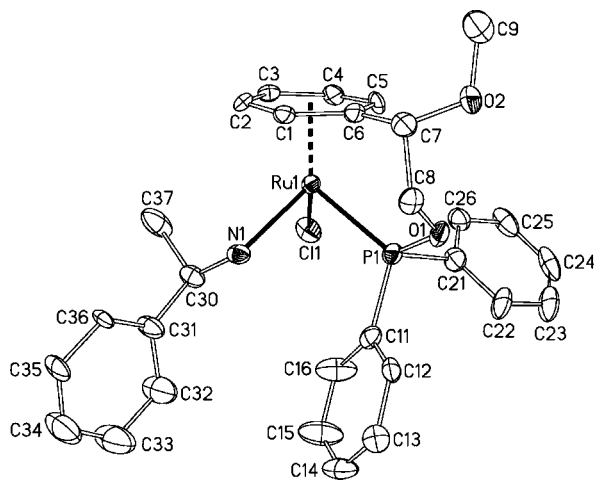


Figure 4. Thermal ellipsoid plot (50% probability) of the molecular structure of the diastereomeric complex cation of PF_6^- salt **9R**: (S_{Ru},R,R), methoxy group “out of plane”; hydrogen atoms omitted for clarity; selected bond distances and angles, see Table 5.

Table 5. Selected Bond Distances and Angles of the Complex Cation of PF_6^- Salt **9R**

distance	[Å]	angle	[deg]
Ru(1)–Cl(1)	2.413(2)	Cl(1)–Ru(1)–P(1)	86.55(5)
Ru(1)–P(1)	2.293(2)	Cl(1)–Ru(1)–N(1)	87.5(2)
Ru(1)–N(1)	2.183(4)	P(1)–Ru(1)–N(1)	91.2(2)
Ru(1)–C(1)	2.213(5)	P(1)–Ru(1)–C(2)	151.5(2)
Ru(1)–C(2)	2.281(5)	P(1)–Ru(1)–C(3)	155.7(2)
Ru(1)–C(3)	2.286(5)	N(1)–Ru(1)–C(4)	149.3(2)
Ru(1)–C(4)	2.207(5)	N(1)–Ru(1)–C(5)	158.5(2)
Ru(1)–C(5)	2.211(5)	Cl(1)–Ru(1)–C(1)	158.6(2)
Ru(1)–C(6)	2.222(5)	Cl(1)–Ru(1)–C(6)	151.1(2)
P(1)–O(1)	1.625(4)	C(9)–O(2)–C(7)	114.9(5)
C(8)–O(1)	1.433(7)	C(6)–C(7)–O(2)	111.7(5)
C(7)–C(8)	1.507(8)	C(6)–C(7)–C(8)	111.6(5)
C(6)–C(7)	1.524(7)	C(7)–C(8)–O(1)	111.4(5)
C(7)–O(2)	1.419(7)	C(8)–O(1)–P(1)	120.3(3)
C(9)–O(2)	1.418(8)	O(1)–P(1)–Ru(1)	112.7(2)
N(1)–C(30)	1.506(7)	Ru(1)–N(1)–C(30)	121.6(3)

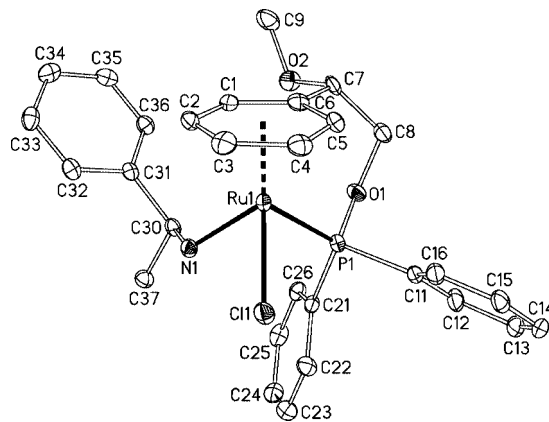


Figure 5. Thermal ellipsoid plot (50% probability) of the molecular structure of the diastereomeric complex cation of PF_6^- salt **10S**: (S_{Ru},S,R), methoxy group “in plane”; hydrogen atoms omitted for clarity; selected bond distances and angles, see Table 6.

Table 6. Selected Bond Distances and Angles of the Complex Cation of PF_6^- Salt **10S**

distance	[Å]	angle	[deg]
Ru(1)–Cl(1)	2.4038(7)	Cl(1)–Ru(1)–P(1)	87.61(3)
Ru(1)–P(1)	2.2928(7)	Cl(1)–Ru(1)–N(1)	81.83(7)
Ru(1)–N(1)	2.150(2)	P(1)–Ru(1)–N(1)	89.08(7)
Ru(1)–C(1)	2.184(3)	P(1)–Ru(1)–C(2)	153.65(8)
Ru(1)–C(2)	2.261(3)	P(1)–Ru(1)–C(3)	156.38(8)
Ru(1)–C(3)	2.266(3)	N(1)–Ru(1)–C(4)	150.82(10)
Ru(1)–C(4)	2.211(3)	N(1)–Ru(1)–C(5)	159.89(9)
Ru(1)–C(5)	2.218(3)	Cl(1)–Ru(1)–C(1)	156.07(8)
Ru(1)–C(6)	2.202(3)	Cl(1)–Ru(1)–C(6)	156.06(7)
P(1)–O(1)	1.621(2)	C(9)–O(2)–C(7)	113.1(2)
C(8)–O(1)	1.445(4)	C(6)–C(7)–O(2)	110.2(2)
C(7)–C(8)	1.527(4)	C(6)–C(7)–C(8)	114.2(2)
C(6)–C(7)	1.527(4)	C(7)–C(8)–O(1)	113.2(2)
C(7)–O(2)	1.428(3)	C(8)–O(1)–P(1)	119.3(2)
C(9)–O(2)	1.432(4)	O(1)–P(1)–Ru(1)	112.74(9)
N(1)–C(30)	1.504(3)	Ru(1)–N(1)–C(30)	124.8(2)

Results and Discussion

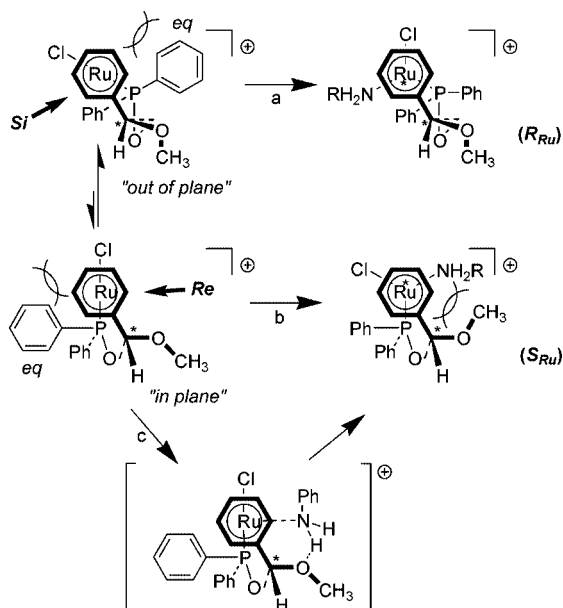
Synthesis of Complex 6. Preparation of chiral complex **6** is based on (*S*)-mandelic acid (**1**), which was converted into (*2S*)-2-methoxy-2-phenylethanol (**2**) according to published procedures^{7a-d} (Scheme 1). Base-promoted alcoholysis of **2** afforded the target *ansa*-phosphinite arene ligand **3**. Its σ -complexation to ruthenium was achieved with η^6 -methylbenzoate ruthenium dichloride dimer **4**^{5d,e} followed by an arene exchange reaction. Formation of stable $\sigma(P)$ -complex **5** was monitored by ³¹P NMR. After completion of this step, the solution was heated at 120 °C in a pressure Schlenk tube until the C-phenyl group of **3** substituted the η^6 -methylbenzoate ligand of **5** to form neutral (*R*)-[$\sigma(P):\eta^6\text{-}(ansa\text{-phosphinite})\text{benzene}]\text{Ru(II)Cl}_2$ (**6**) in 62% isolated yield (Figure 1).

The methoxy group of **6** adopts rather an “out-of-plane” conformation with respect to the η^6 -arene Ru(II) fragment, whereas the methyl group in the analog *ansa*-phosphine complex occupies a clear *exo* position.^{5d,8a} The Ru(1)–Cl bond lengths of 2.41 Å are elongated, but the Ru(1)–P(1) bond, at 2.29 Å, is slightly shortened (Table 1). Therefore it can be concluded that for **6** the Ru(1)–Cl bonds are weakened, while the Ru(1)–P(1) bond is strengthened. Also the *trans* influence of the phosphinite ligand on C(2) and C(3) of the η^6 -arene ligand seems to be retarded. These differences point to a phosphinite moiety, which is a slightly weaker π -acceptor but a little better σ -donor than related tethered phosphine ligand functions.

Table 7. Crystallographic Data, Data Collection, and Refinement Details of Neutral Complex **6** and PF₆⁻ Salts **7S**, **8**·(MeOH)_{0.5}, **9R**·MeOH, and **10S** Measured at 100 K

	6	7S	8 ·(MeOH) _{0.5}	9R (MeOH)	10S
empirical formula	C ₂₁ H ₂₁ Cl ₂ O ₂ PRu	C ₂₇ H ₂₆ ClF ₆ NO _{2.5} P ₂ Ru	C _{27.5} H ₂₉ ClF ₇ NO _{2.5} P ₂ Ru	C ₃₀ H ₃₆ ClF ₆ NO ₃ P ₂ Ru	C ₂₉ H ₃₂ ClF ₆ NO _{2.5} P ₂ Ru
mol weight	508.35	710.99	745.00	771.06	739.04
cryst syst	monoclinic	monoclinic	triclinic	orthorhombic	monoclinic
space group	<i>P</i> ₂ ₁ (no. 4)	<i>P</i> ₂ ₁ (no. 4)	<i>P</i> 1 (no. 1)	<i>P</i> ₂ ₁ <i>2</i> ₁ (no. 19)	<i>P</i> ₂ ₁ (no. 4)
<i>a</i> (Å)	9.7487(3)	9.364(1)	10.9667(9)	10.554(2)	9.4734(4)
<i>b</i> (Å)	9.9464(7)	15.414(2)	10.9759(7)	13.150(1)	16.2505(8)
<i>c</i> (Å)	10.4269(6)	9.544(2)	14.2777(7)	23.409(4)	9.7948(7)
α (deg)	90	90	76.588(5)	90	90
β (deg)	91.709(3)	93.54(1)	89.832(5)	90	91.773(6)
γ (deg)	90	90	60.962(5)	90	90
<i>V</i> (Å ³)		1374.9(4)	1449.4(2)	3248.8(9)	1507.2(2)
<i>Z</i>	2	2	2	4	2
ρ (g/cm ³) (calcd)	1.670	1.717	1.707	1.576	1.628
μ (mm ⁻¹)	1.133	0.852	0.819	0.730	0.781
<i>F</i> (000)	512	716	750	1568	748
abs corr	SADABS	SADABS	numerical	numerical	SADABS
<i>T</i> _{min} ; <i>T</i> _{max}	0.871; 0.923	0.801; 0.960	0.790; 0.894	0.773; 0.930	0.759; 0.860
2θ interval (deg)	6.0 ≤ 2θ ≤ 57.4	6.8 ≤ 2θ ≤ 55.8	6.3 ≤ 2θ ≤ 55.8	6.4 ≤ 2θ ≤ 54.2	6.5 ≤ 2θ ≤ 57.1
no. of coll refls	30 994	38 631	43 503	32 057	39 743
no. of indep refls	5214	6543	12743	7093	7577
no. of obsd refls <i>F</i> ₀ ≥ 4σ(<i>F</i>)	4541	6135	10553	6386	6701
no. of ref params	246	362	761	456	379
wR2 (all data)	0.0614	0.0451	0.0792	0.1114	0.0623
R1 (<i>F</i> ₀ ≥ 4σ(<i>F</i>))	0.0302	0.0219	0.0359	0.0527	0.0306
Goof on <i>F</i> ²	0.826	1.001	1.022	1.173	1.075
abs struct param	-0.03(3)	0.01(2)	-0.01(2)	0.01(4)	-0.01(2)
max.; min. electr dens	0.567; -0.785	0.293; -0.432	0.834; -0.535	0.980; -1.153	0.509; -0.501

Scheme 2. Permutations of Nucleophilic Ligand Attack on Proposed Cationic 16 VE Ru(II) Intermediates (top view on η⁶-arene moieties): (a) Sterically Preferred Attack of Incoming Aniline on Cationic 16 VE Intermediate in "Out-of-Plane" Conformation, (b) Sterically Preferred Attack of Incoming Aniline on Cationic 16 VE Intermediate in "in Plane" Conformation, (c) Proposed Delivery Effect via H-Bond Formation Leading to the Preferred Formation of **7S** and **8S** under the Reaction Conditions



Diastereoselective Substitution Reactions. Complex **6** was subjected to nucleophilic substitution reactions of one chloride ligand at the diastereotopic Ru(II) center with primary anilines and aliphatic chiral amines, to generate complex salts with an additional chiral center at the metal (Scheme 1).^{8b} The reactions were performed with NaPF₆ as chloride-trapping reagent. Only for aniline and *p*-fluoroaniline PF₆ salts **7** and **8** could a significant excess of the diastereomers **7S** and **8S** be determined

in the reaction mixtures by NMR spectroscopy, but not for **9** and **10**, with (*R*)- and (*S*)-1-phenylethylamine ligands. A configurational lability of the chiral Ru(II) center of the complex salts was indicated when working up the compounds. **7S** and

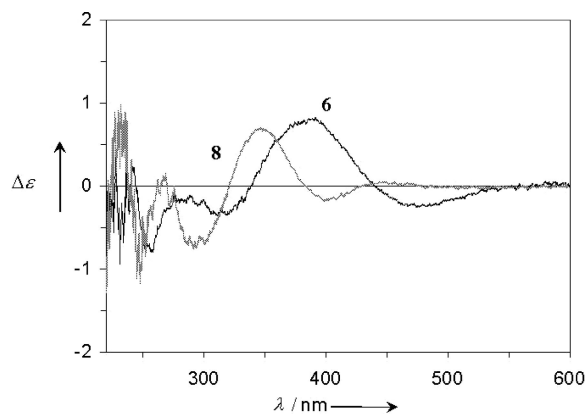
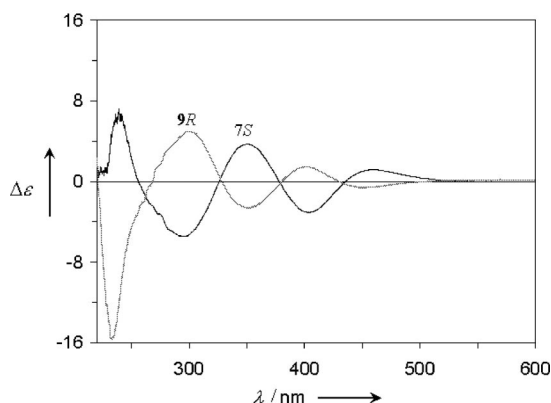
**Figure 6.** CD spectra of complex **6** (bold line) and salt **8** (nonbold line) in MeOH.**Figure 7.** CD spectra of complex salts **7S** (bold line) and **9R** (nonbold line) in MeOH.

Table 8. Main UV and CD Spectral Features in Methanol of Compounds **6**, **7S**, **8**, **9R**, and **10**

compound	UV $\lambda(\epsilon \times 10^{-3})$	CD $\lambda(\Delta\epsilon)$
6	473(0.24), 353(1.5), 228sh(21.4)	475(-0.25), 389(0.81), 316(-0.32), 258(-0.79)
7S	349(1.5), 276sh(5.9), 245sh(16.0)	461(1.18), 404(-3.05), 350(3.72), 295(-5.45), 240(6.55)
8	350(1.5), 275sh(6.2), 246sh(15.2)	444(0.04), 403(-0.17), 345(0.69), 294(-0.75), 267(0.11), 248(-1.2)
9R	340sh(1.27), 323(1.38), 228(22.81)	452(-0.66), 403(1.43), 352(-2.68), 301(4.91), 233(-15.62)
10	327(1.38), 228(20.67)	419(-0.41), 346(0.44), 301sh(-0.44), 230(-4.07)

8S epimerize at the metal center, and longer handling of diastereomeric mixture **9** resulted in an enrichment of diastereomer **9R**. The ^{31}P NMR signal assignments to particular diastereomers of **7**–**9** were concluded from correlations with the ^1H NMR spectra of the reaction samples, of the crude, and of the purified products. This was confirmed with NOE measurements and X-ray crystal structure analysis (*vide infra*), but the approach failed for **10**, because no de was observed in that case. Salts **7**–**9** formed well-defined crystalline materials suitable for X-ray structure analysis: **7** as **7S** exclusively (Figure 2, Table 2), **8** in a 1:1 ratio of **8S** and **8R** (Figure 3, Tables 3, 4), and **9** as **9R** only again (Figure 4, Table 5). **10** precipitated regularly as a 1:1 mixture of diastereomers as indicated by NMR and CD, but some single crystals of **10S** could be sorted out manually (Figure 5, Table 6). The preservation of the original *R* configuration of the chiral benzylic center of the *ansa* chain was confirmed in all cases, so the benzyl stereogenic center of the ligand is stable with respect to all chemical manipulations applied. A complete set of crystallographic data are summarized in Table 7.

Unlike **7** and **8**, diastereomer **9R** did not epimerize over periods of weeks in a number of solvents tested. The configurative stability of **9R** resembles that of the analogue ($R_{\text{Ru}}, R_{\text{C}}$)-enantiomers of the [[$\sigma(P)$]: η^6 -(ansa-phosphine)benzene}Ru(II)Cl(NH₂R)]⁺ complexes described earlier.^{5d} As for neutral **6**, the molecular structure of the cation of **9R** in the solid state (Figure 4) is characterized by an “out-of-plane” orientation of the methoxy group. This stabilizes a chairlike conformation of the *ansa* chain, which in turn geometrically fixes the phosphinite coordination mode in a way that one phenyl group adopts an *axial* (*ax*) and the other an *equatorial* (*eq*) position. Coordinating from the *si* face, the amine ligand adopts the position with the longest distance to the equatorial phenyl ring with a minimum of steric repulsion. In contrast to that, aniline salt **7S** epimerized within hours at ambient temperature in acetone-*d*₆ to yield mixtures of **7R** and **7S**. The molecular structure of the cation of **7S** with its *S* configuration of the Ru(II) center (Figure 2) differs clearly from **9R** and **6** by a sterically disfavored “in-plane” conformation of the methoxy group. Again, a chairlike conformation of the *ansa* chain is observed, but with an enhanced strain if compared to the complex cations with *R* configurations of the metal atom. The phosphinite coordination geometry is also fixed in an “ax-*eq*” mode, but with opposite diastereotopic orientation causing the amine to coordinate from the *Re* side here, to reduce steric repulsion. These stereochemical results are completed by the crystal structure of **8** (Figure 3, Table 4, Table 5), where both diastereomers **8S** and **8R** are present as independent complex cations in the unit cell. As one would assume, diastereomer **8S** adopts the same conformation as **7S** and **10S**, whereas **8R** is a close relative of **9R**. In all investigated cases of ($S_{\text{Ru}}, R_{\text{C}}$) diastereomers, the methyl group of the methoxy moiety “turns away” from the η^6 -arene ring, leaving the main steric interactions to the oxygen atom alone. The higher volume of a methyl group with respect to an oxygen atom thus generates the driving force for the highly preferred formation of ($S_{\text{Ru}}, R_{\text{C}}$) over ($R_{\text{Ru}}, R_{\text{C}}$) diastereomers of the analogue [[$\sigma(P)$]: η^6 -(ansa-phosphine)benzene}Ru(II)Cl(NH₂R)]⁺ complex cations.^{5d} Com-

plementarily it can be understood why the configurationally labile diastereomer **7S** can be isolated at all.

Contrary and unexpected to the analogue phosphine systems the sterically less favored diastereomers **7S** and **8S** are formed in excess in the reaction mixture; in no case was the formation of the ($R_{\text{Ru}}, R_{\text{C}}$) diastereomers preferred under kinetic conditions. Only 1:1 diastereomer mixtures for **9** and **10** resulted; thus the direction of the kinetic diastereoselectivity points to a clear dependence on starting material **6**, while its magnitude is determined by the nature of the amine ligand. For the amine substitution an $S_{\text{N}}1$ -type reaction mode via cationic 16 VE [[$\sigma(P)$]: η^6 -(ansa-phosphinite)benzene}Ru(II)Cl]⁺ intermediates by loss of one chloride ligand can be considered,^{5d,9} which are closely related to the molecular structures of the tethered species found in this study. This suggests “out-of-plane” and “in-plane” conformations of the methoxy groups again, and the sterically preferred “out-of-plane” conformation is believed to dominate for the 16 VE intermediates in the reaction solution. Due to the orientation of the phenyl substituents of the phosphorus atom, this conformer promotes a sterically favored *si* face attack of the incoming amine ligand, which in turn should lead to the formation of the more stable ($S_{\text{Ru}}, R_{\text{C}}$) amine complex (Scheme 2, pathway a). The energetically discriminated “in-plane” conformation of the intermediate, however, would lead to a preferred *re* attack of the incoming amine ligand and thus to the less stable ($S_{\text{Ru}}, R_{\text{C}}$) complex cation (pathway b). These considerations would account for the S_{Ru} diastereomers only as the minor component; thus another interaction is required to explain their dominance for **7** and **8**. A delivery effect as observed for chromium(0) tricarbonyl η^6 -arene complexes¹⁰ serves as the model. The oxygen atom of the methoxy group has the potential to form a hydrogen bridge with the approaching amine, which can only be delivered to the Ru(II) center in the case of an “in-plane” conformation (pathway c). The effect should be controlled by the strength of the resulting O–H–N hydrogen bond, which is a function of the amino protons’ acidity. The acidities of aniline ($\text{pK}_{\text{a}} \approx 25$) and *p*-fluoroaniline

(7) (a) Dickman, M.; Jones, J. B. *Bioorg. Med. Chem.* **2000**, 1957. (b) McKenzie, A.; Wren, H. *J. Chem. Soc.* **1910**, 97, 484. (c) Guanti, G.; Nariano, E.; Banfi, L.; Scolastico, C. *Tetrahedron Lett.* **1983**, 24, 817. (d) Christoffers, J.; Rössler, U. *Tetrahedron: Asymmetry* **1998**, 9, 2349. (analogue).

(8) (a) Note the denotation of the absolute configuration of the chiral center in the *ansa* chain of **6** formally changes to (*R*). (b) The stereochemical descriptors for the (π -arene)RuL₃ units of this paper follow the recommendations of: Bünzli-Trepp, U. *Handbuch für die systematische Nomenklatur der Organischen Chemie, Metallorganische Chemie und Koordinationschemie*; Logos Verlag: Berlin, 2001; Part A 6.4(d).

(9) (a) Carmona, D.; Lamata, M. P.; Oro, L. A. *Eur. J. Inorg. Chem.* **2002**, 2239. (b) Davenport, A. J.; Davies, D. L.; Fawcett, J.; Garratt, S. A.; Russel, D. R. *J. Chem. Soc. Chem. Commun.* **1999**, 2331. (c) Brunner, H.; Neuhierl, T.; Nuber, B. *Eur. J. Inorg. Chem.* **1998**, 1877. (d) Carmona, D.; Vega, C.; Lahoz, F. J.; Elipse, S.; Oro, L. A.; Lamata, P. M.; Viguri, F.; Garcia-Correas, R.; Cativiela, C.; Lopez-Rarn de Viu, M. P. *Organometallics* **1999**, 18, 3364. (e) Brunner, H.; Zwack, T. *Organometallics* **2000**, 19, 2423. (f) Faller, J.; Grimmond, B. J.; Curtis, M. *Organometallics* **2000**, 19, 5174. (g) Arena, C. G.; Galamia, S.; Faraone, F.; Graiff, C.; Tiripicchio, A. *J. Chem. Soc., Dalton Trans.* **2000**, 3149.

(10) (a) Uemura, M.; Kobayashi, T.; Isobe, K.; Minami, T.; Hayashi, Y. *J. Org. Chem.* **1986**, 51, 2859. (b) Ganter, C.; Brassat, L.; Ganter, B. *Chem. Ber. Recl.* **1997**, 130, 659.

allow the delivery effect to proceed, but vanishes in the case of 1-phenylethylamine ($pK_a \approx 34$). Due to a missing partner for the formation of hydrogen bridges with incoming amines, the chloride substitution results on tethered arene phosphine and phosphetane ruthenium complexes are not influenced that way.^{5,d,e}

NMR Study. The assignments of the ^1H NMR and ^{13}C NMR signals belonging to the particular diastereomers of mixtures **8S/8R** and **10S/10R** were accomplished by similarity correlation of NOE measurements of diastereomerically pure **7S** and is worked out in detail in the Supporting Information. The distinct assignable NOE effects to particular diastereomers give clear evidence that the conformational flexibility of the particular *ansa* chains is highly restricted.

Circular Dichroism Study. UV and CD spectra (210–600 nm range, MeOH) of compounds **6**, **7S**, **8**, **9R**, and **10** were recorded (Figures 6 and 7, Table 8), in order to get further information about absolute and relative configurations of these complexes in solution and deeper insight into the epimerization process of **7S**. The UV spectrum of **6** (Table 8) shows two absorption bands at 473 and 353 nm, which can be ascribed to either d–d or MLCT transitions,¹¹ followed by a more intense band at 228 nm. The CD spectrum of **6** (Figure 6) shows four Cotton effects, at 475 nm ($\Delta\epsilon -0.25$), 389 nm ($\Delta\epsilon 0.81$), 316 nm ($\Delta\epsilon -0.32$), and 258 nm ($\Delta\epsilon -0.79$), which are at different wavelength than the UV absorptions, except for the lower energy band. All CD signals can be related to the chiral metal η^6 -arene chromophore, because the free aromatic ligand exhibits only very weak CD signals in that range.^{12a}

Interestingly, the same sequence of CD bands with nearly the same intensities and wavelengths is displayed by structurally related Ru(II) η^6 -arene complexes^{1f,3b} with a benzylic chiral center. An empirical correspondence between the sign of the CD bands and the absolute configuration of the benzylic carbon atom is observed in all these compounds. The CD spectrum of diastereomerically pure salt **7S** (>99% de) displays Cotton effects (Figure 7) at 461 nm ($\Delta\epsilon 1.18$), 404 nm ($\Delta\epsilon -3.05$), 350 nm ($\Delta\epsilon 3.72$), 295 nm ($\Delta\epsilon -5.45$), and 240 nm ($\Delta\epsilon 6.55$), which are about 5 times more intense than those in the spectrum of **6**. We relate them to a chiroptical dominance of the *S*-configured chiral metal center, which overlaps the signals of the chiral arene chromophore, confirming a high diastereomeric purity of **7S** in freshly prepared methanol solution. The spectrum rerecorded after some days resembles that of a 1:1 diastereomeric mixture of **8** or neutral **6** (Figure 6), with disappearance of the dominating influence of the metal. This proves the configurational instability of the metal center of **7S** in several solvents again and a complete retention of the absolute configuration at the benzylic carbon atom by an independent method. The CD spectrum of **8** is characterized by the same band sequence of **6**, with the same sign and signal intensity, although with a 30 nm hypsochromic shift, due to the presence of an amine ligand at the metal, thus confirming complete epimerization at the metal center and retention of the absolute configuration at the benzylic carbon. The CD spectrum of **9R** (>99% de, Figure 7) is in an almost mirror image relationship with the one of **7S**, revealing a spectral dominance of the chiral metal atoms and their opposite absolute configurations. Probably, only the strong negative Cotton effect at 233 nm can result from a partial contribution of the chiral amine chromophore, being in correspondence to the absorption band at 228 nm in the UV spectrum, which could be ascribed to a bathochromic shifted aromatic $^1\text{L}_a$ transition of the amine.^{12b} Differently from **7S**,

the CD spectrum of **9R** appeared unchanged even after one month of standing, revealing the high configurational stability of this complex in methanol solution. Finally, the CD spectrum of **10** (1:1 diastereomeric mixture, Table 8) appeared quite similar in intensity, position, and sign of the CD bands to the one of **8**, leading to the same interpretations.

In conclusion, this CD analysis shows that (i) as expected, in all the complexes examined the absolute configuration at the benzylic chiral center is retained; (ii) the complex salts **7S** and **9R** have opposite absolute configuration at the chiral Ru(II) centers; (iii) the samples of **8** and **10** show complete epimerization at the chiral metal center; (iv) complex **7S** epimerizes at the metal center in methanol solution, while under the same conditions **9R** is configurationally stable.

Catalytic Transfer Hydrogenation of Acetophenone. Compounds **7S** and **9R** were tested as precatalysts in the transfer hydrogenation reaction of acetophenone with 2-propanol to yield asymmetric 1-phenylethanol in the presence of strong bases. A limited solubility of the salts in the reaction mixtures required an adjustment of the molar *i*-PrOH/acetophenone ratio, as observed earlier for the analogous (*ansa*-phosphine) and (*ansa*-phosphetane) ruthenium complex salts.^{5,d,e} The reactivity of both catalysts was fair, but the poor (**7S**, 9% ee (*R*)-1-phenylethanol) or even completely absent enantioselectivity in the case of **9R** points to a general lack of suitability of the investigated tethered complex salts as catalysts for enantioselective transfer hydrogenation.

Conclusions

The presented studies on diastereomeric *ansa* complex salts **7–10** revealed the following facts that determine the configurational stability of the complex cations: (i) The configurational stabilization of the chiral Ru(II) centers is based on the fixed diastereotopic “*ax-eq*” coordination mode of the diphenyl phosphinite moiety via steric interaction of the *eq* phenyl rings with the amine ligands, for both, the ($S_{\text{Ru}}, R_{\text{C}}$) and ($R_{\text{Ru}}, R_{\text{C}}$) diastereomers. (ii) The chairlike conformation of the *ansa* chain is not flexible for both diastereomers. Its diastereotopic orientation is determined by the absolute configuration of the chiral Ru(II) center. (iii) The configurational metastability of the ($S_{\text{Ru}}, R_{\text{C}}$) diastereomers is evoked by the unfavored “*in-plane*” conformation of the methoxy group. The ($R_{\text{Ru}}, R_{\text{C}}$) diastereomers of the [amino{ $\sigma(P):\eta^6$ -[(2'-(*P,P*-diphenylphosphinoxy)-1'-methoxyethyl)benzene]}chloroRu(II)]⁺ complex cations are therefore thermodynamically favored and configurationally stable. In contrast to that, Faller interprets the reason for his slowly epimerizing [{ $\sigma(P):\eta^6$ -(*ansa-P*)benzene}Ru(II)(P \cap S)] complex family as the hemilability of the sulfide ligand function of the P \cap S chelate.^{4g} On the other hand, for Brunner's Mn(I),¹³ Gladysz' Re(I),¹⁴ and Davies' Fe(II) η^5 -Cp complexes¹⁵ configurational stabilization could be achieved exclusively by electronic control. We demonstrated that chiral Ru(II) η^6 -arene complexes require for that purpose additional steric stabilization.

(12) (a) Smith, H. E. *Chem. Rev.* **1998**, *98*, 1709. (b) Johnson, W. C., Jr.; Fontana, L. P.; Smith, H. E. *J. Am. Chem. Soc.* **1987**, *109*, 3361.

(13) (a) Brunner, H. *Angew. Chem., Int. Ed.* **1969**, *8*, 382. (b) Brunner, H. *Adv. Organomet. Chem.* **1980**, *18*, 151. (c) Brunner, H.; Langer, M. *J. Organomet. Chem.* **1975**, *87*, 223. (d) Brunner, H. *J. Organomet. Chem.* **1975**, *94*, 189. (e) Brunner, H.; Aclasis, J. A. *J. Organomet. Chem.* **1976**, *104*, 347.

(14) (a) Gladysz, J. A.; Boone, B. J. *Angew. Chem., Int. Ed.* **1997**, *36*, 550, and references therein. (b) Wong, W. K.; Tam, W.; Strouse, C. E.; Gladysz, J. A. *J. Chem. Soc., Chem. Commun.* **1979**, 530. (c) Astakhova, I. S.; Johansson, A. A.; Semion, V. A.; Struchkov, Y. T.; Anibsimov, K. N.; Kolobova, N. E. *J. Chem. Soc., Chem. Commun.* **1969**, 488. (d) Lukchart, C. M.; Zeile, J. V. *J. Am. Chem. Soc.* **1976**, *98*, 2365.

(11) (a) Peacock, R. D.; Stewart, B. *Coord. Chem. Rev.* **1982**, *46*, 129. (b) Ziegler, M.; Von Zelewsky, A. *Coord. Chem. Rev.* **1998**, *177*, 257.

Right in line with observing a significant configurational lability of aniline salt **7**, isolated diastereomer **7S** failed to produce useful ee values when being used as an enantioselective transfer hydrogenation catalyst. Not yet fully understood is the complete failure of the configurationally more stable diastereomer **9R** to produce any observable enantioselectivity in that catalytic reaction, but different conditions for an epimerization of the chiral metal center of the cationic 18 VE precatalysts and their catalytically active 16 VE counterparts are obvious. In both cases, the chosen tether between arene and phosphinite donor functions of the ligand seems not to be rigid enough to stabilize the decisive intermediates of the catalytic transfer hydrogenation. Therefore, the design of potentially highly enantioselective, chiral *ansa*-linked Ru(II) η^6 -arene transfer hydrogenation catalysts has to be changed principally. Such work is in progress.¹⁶

Experimental Section

General Procedures. All reactions were carried out under an atmosphere of dry nitrogen using conventional Schlenk techniques. All workups were performed in air, and all substances prepared are stable in air, including the Ru(II) η^6 -arene complexes, which are only slightly air-sensitive in solution. Solvents and chemicals were purchased from Acros, Aldrich, Merck, and Strem. The following solvents and reagents were dried and distilled in an atmosphere of nitrogen prior to use: chlorodiphenylphosphine, NEt₃, aniline, *p*-fluoroaniline. Drying agents: CH₂Cl₂ and CDCl₃—calcium hydride; THF—sodium/benzophenone; MeOH—magnesium. All other solvents and reagents were employed as received. Silica gel F 60 for flash chromatography (FC) was purchased from Fluka or Merck. Thin-layer chromatography (TLC) was performed on Merck F 60 silica plates with a 364 nm fluorescence indicator and used for the determination of the *R_f* values. NMR spectra were recorded on Jeol FT-JNM-EX 270 (270 MHz), Bruker AMX 300 (300 MHz), Jeol FT-JNM-LA 400 (400 MHz), and Jeol A 500 (500 MHz) spectrometers in deuterated solvents and referenced to the residual ¹H or ¹³C{¹H} signals of the particular solvent. 2D spectra were not symmetrized. ³¹P{¹H} NMR spectra were referenced to external 85% H₃PO₄ or to the anion PF₆[−] of salts **7–10**. Mass spectra were recorded on a Varian MAT 212 spectrometer. Elemental analyses were performed using a Carlo Erba elemental analyzer model 1108. Absorption and circular dichroism spectra were recorded on a JASCO J-600 spectropolarimeter at RT in MeOH, using concentrations of about 1 × 10^{−3} M. During the measurement, the instrument was thoroughly purged with nitrogen. Polarimetric measurements were performed on a Perkin-Elmer 341 polarimeter. Melting points were determined on a Büchi 530 melting point apparatus and are not corrected. Compounds **2**^{7a–d} and **4**^{5d,e} were prepared as reported.

(+)-(2S)-P-(2-Methoxy-2-phenylethoxy)-P,P-diphenylphosphine (**3**). To 5.72 g (37.6 mmol) of **2** and 6.50 mL (4.72 g, 46.6 mmol) of NEt₃ in 200 mL of THF was added dropwise 7.50 mL (9.22 g, 41.8 mmol) of chlorodiphenylphosphine within 5 min at RT, and triethylammonium hydrochloride started to precipitate out immediately. The mixture was then stirred for 12 h at 60 °C. Workup: To the reaction mixture were added 15 mL of NEt₃ and then ca. 10 g of hydrated silica gel to absorb most of excess chlorodiphenylphosphine. The suspension was stirred for 10 min and filtered. Removal of all volatiles by RV and under HV furnished 13.05 g of crude **2** as an oil, which was purified by FC (hexanes: EtOAc = 3:1 + 5% NEt₃, *R_f*(**2**) = 0.28, *R_f*(**3**) = 0.59). HV drying yielded 10.79 g of pure **3** (32.1 mmol, 85%) as a clear, colorless oil. [α]_D²³ +39.8 (CHCl₃, *c* 0.18). ¹H NMR (270 MHz, CDCl₃): δ 7.49–7.20 (series of m, 15H, *Ph*-CH-, -PPh₂); 4.36 (dd, ³J_{H,H} = 7.8, ³J_{H,H} = 3.8, 2H, -CH-); 4.09–3.87 (2 not res. ddd, 2H, -CH₂-); 3.13 (s, 3H, -OCH₃). ¹³C{¹H} NMR (68 MHz, CDCl₃): δ 142.19 (d, ¹J_{C,P} = 12.1, 1-C of -PPh₂); 141.93 (d, ¹J_{C,P} = 12.1, 1-C of -PPh₂); 138.38 (1-C of *Ph*-CH-); 130.42 (d, ²J_{C,P} = 4.7, 2- or 6-C of -PPh₂); 130.10 (d, ²J_{C,P} = 4.7, 6- or 2-C of -PPh₂); 129.06 (4-C of *Ph*-CH-); 128.35 (3,5-C of *Ph*-CH-); 128.17 (d, ³J_{C,P} = 1.4, 3- or 5-C of -PPh₂); 128.07 (d, ³J_{C,P} = 1.4, 5- or 3-C of -PPh₂); 127.94 (4-C of -PPh₂); 126.98 (4-C of *Ph*-CH-); 83.90 (d, ³J_{C,P} = 5.9, -CH-); 74.39 (d, ²J_{C,P} = 17.8, -CH₂-); 56.83 (-CH₃). ³¹P{¹H} NMR (109 MHz, CDCl₃): δ 116.47 (s, 1P). FD⁺-MS (CH₂Cl₂); *m/z* (%) 336 (100) [M⁺]. C₂₁H₂₁O₂P (336.37): calcd C 74.99, H 6.29; found C 74.78, H 6.27.

(1R)-Dichloro{ $\sigma(P)$ }: η^6 -[(2-(P,P-diphenylphosphinoxy)-1-methoxyethyl)benzene]ruthenium(II) (**6**). *Caution! Autoclave burst protection equipment mandatory, the pressure Schlenk tube must be capable of withstanding a pressure of 120 bar.* A 1.773 g (2.88 mmol) portion of methylbenzoate ruthenium dichloride complex dimer **4** and 2.251 g (6.69 mmol) of **3** were stirred in a pressure Schlenk tube in 30 mL of CH₂Cl₂ and 1.5 mL of THF at RT. Within 20 min the reaction mixture turned to a clear, deep red solution and the state of formation of σ -complex **5** can be monitored by ³¹P{¹H} NMR (109 MHz, CDCl₃): δ 109.95 (s, 1P). Full conversion of **5** into target complex **6** requires 11 h stirring at 120 °C and can be controlled by ³¹P{¹H} NMR again. *Caution! Before opening, the pressure Schlenk tube must cool down to RT slowly.* Workup: The reddish-brown reaction mixture was filtered through cellulose, and the solvents were removed by RV. The slimy crude product was washed with Et₂O and redissolved in THF, and the solvent was removed by RV, giving a microcrystalline product, which was recrystallized from a minimum of hot THF down to -30 °C. After filtration from the mother liquor the product was washed consecutively with small amounts of cold THF, MeOH, and Et₂O and dried on air to yield 1.826 g (3.59 mmol, 62%) of **6**, including additional material from the mother liquors. Crystals suitable for X-ray crystal structure analysis were grown by slow solvent evaporation from CH₂Cl₂ solution. Mp: 188–190 °C (dec). [α]_D²³ +7.4 (CH₂Cl₂, *c* 0.0034). ¹H NMR (270 MHz, CDCl₃): δ 7.88–7.74 (m, 4H, 2,6-H of -PPh₂); 7.41–7.27 (m, 6H, 3,4,5-H of -PPh₂); 6.47 (pseudo t, 1H, 3- or 5-H of η^6 -Ph); 6.06 (pseudo t, 1H, 5- or 3-H of η^6 -Ph); 5.64–5.56 (m and not res. d, 2H, 2- or 6-H and 4-H of η^6 -Ph); 5.25 (d, ³J_{H,H} = 5.1, 1H, 6- or 2-H-C of η^6 -Ph); 4.37–4.18 (2 not res. ddd, 2H, -CH₂-); 4.12 (dd, ³J_{H,H} = 5.3, ³J_{H,H} = 3.1, 1H, -CH-); 3.41 (s, 3H, -CH₃). ¹³C{¹H} NMR (68 MHz, CDCl₃): δ 136.46 (d, ¹J_{C,P} = 57.1, 1-C of -PPh₂); 134.51 (d, ¹J_{C,P} = 56.4, 1-C of -PPh₂); 131.43 (d, ²J_{C,P} = 9.6, 2,6-C of -PPh₂); 131.27 (d, ²J_{C,P} = 9.6, 6- or 2-C of -PPh₂); 130.97 (d, ⁴J_{C,P} = 2.7, 4-C of -PPh₂); 130.82 (d, ⁴J_{C,P} = 2.6, 4-C of -PPh₂); 128.04 (d, ³J_{C,P} = 11.0, 3,5-C of -PPh₂); 127.78 (d, ³J_{C,P} = 11.0, 3,5-C of -PPh₂); 104.05 (d, ²J_{C,P} = 9.6, 3- or 5-C of η^6 -Ph); 93.60 (d, ²J_{C,P} = 8.0, 5- or 3-C of η^6 -Ph); 90.56 (1-C of η^6 -Ph); 86.97 (4-C of η^6 -Ph); 86.91 (6- or 2-C of η^6 -Ph); 85.05 (2- or 6-C of η^6 -Ph); 75.64 (d, ³J_{C,P} = 1.1, -CH-); 70.3 (-CH₂-);

(15) (a) Davies, S. G. *Pure Appl. Chem.* **1988**, *60*, 13, and references therein. (b) Liebeskind, L. S.; Welker, M. E. *Tetrahedron Lett.* **1984**, *25*, 4341. (c) Liebeskind, L. S.; Welker, M. E.; Fengl, R. W. *J. Am. Chem. Soc.* **1986**, *108*, 6328. (d) Davies, S. G.; Dordor-Hedgecock, I. M.; Walker, T. C.; Warner, P. *Tetrahedron Lett.* **1984**, *25*, 2709. (e) Davies, S. G.; Dordor, I. M.; Warner, P. *J. Chem. Soc., Chem. Commun.* **1984**, 956. (f) Ambler, P. W.; Davies, S. G. *Tetrahedron Lett.* **1985**, *26*, 3075–3079. (g) Cameron, A. D.; Baird, M. C. *J. Chem. Soc., Dalton Trans.* **1985**, 2691. (h) Seeman, I. J.; Davies, S. G. *J. Chem. Soc., Dalton Trans.* **1985**, 2692. (i) Heah, P. C.; Patton, A. T.; Gladysz, J. A. *J. Am. Chem. Soc.* **1986**, *108*, 1185, and references therein.

(16) (a) Weber, I.; Heinemann, F. W.; Zenneck, U. *Helv. Chim. Acta* **2007**, *90*, 820. (b) Weber, I.; Heinemann, F. W.; Bakatselos, P.; Zenneck, U. *Helv. Chim. Acta* **2007**, *90*, 834.

(17) (a) Coppens P. In *Crystallographic Computing*; Ahmed, F. R., Ed.; S. R. Hall & C. P. Huber: Munksgaard, Copenhagen, 1970; pp 255–270. (b) SADABS 2.06; Bruker AXS, Inc.: Madison, WI, 2002. (c) SHELXTL NT 6.12; Bruker AXS, Inc.: Madison, WI, 2002.

(18) (a) Wilson, A. J. C., Ed. *International Tables for Crystallography*; Kluwer Academic Publishers: Dordrecht, 1992; Tables 6.1.1.4 (500–502), 4.2.6.8 (219–222), 4.2.4.2 (193–199). (b) Flack, H. D. *Acta Crystallogr.* **1983**, *A39*, 876.

57.56 (–CH₃). ³¹P{¹H} NMR (109 MHz, CDCl₃): δ 125.08 (s, 1P). FD⁺-MS (CH₂Cl₂); *m/z* (%) 509 (100) [M]⁺ with respect to ¹⁰²Ru. C₂₁H₂₁Cl₂O₂PRu (508.35): calcd C 49.62, H 4.16; found C 49.57, H 4.46.

(*S*_{Ru},*1R*)-[*σ*-Chloro{*σ*(*P*):*η*⁶-[(2-(*P,P*-diphenylphosphinoxy)-1-methoxyethyl)benzene]}-*σ*(*N*)-phenylaminoruthenium(II)] Hexafluorophosphate (**7S**). **Representative Procedure.** A 300 mg (0.590 mmol) amount of **6** was dissolved in 4 mL of CH₂Cl₂, followed by addition of 0.10 mL (102 mg, 1.097 mmol) of aniline and 4 mL of MeOH. Then 326 mg (1.941 mmol) of solid NaPF₆ was added in one portion, and the mixture was stirred for 16 h at RT. Before workup >99% de (**7S**) was determined by NMR [³¹P{¹H} NMR (121 MHz, acetone-*d*₆; **7R**): 131.05 (s, 1P); ¹H NMR (270 MHz, acetone-*d*₆; **7R**): 3.40 (s, 3H, –CH₃)]. Workup: After removal of solvents by RV the crude product was dissolved in CH₂Cl₂ and excess NaCl and NaPF₆ were filtrated off over a disposable pipet filled with cellulose filter flakes. The resulting clear yellow to orange solution was evaporated to dryness by RV, and the residue washed free of excess amine with Et₂O inside the round-bottom flask and dried thoroughly under HV to give 504 mg of crude **7** as an orange solid, but with 74% de **7S** by NMR. One-time recrystallization from CH₂Cl₂ at RT down to –30 °C afforded 302 mg (0.425 mmol, 72%) of pure **7S** with >99% de by NMR. The crystals were suitable for X-ray structure analysis. After recrystallization the compound is only sparingly soluble in CH₂Cl₂ and CHCl₃, but slightly in MeOH and moderately in acetone, in which it epimerizes at RT within hours. Acetonitrile causes epimerization of **7S** within minutes, which is followed by *η*⁶-arene ligand decomplexation.

General Procedure for the Preparation of NMR Samples for de Determination. To prevent erroneous de determination, sample preparation and measurement were performed as quickly as possible. Aliquots of 0.1–0.2 mL taken from reaction mixtures were evaporated to dryness by quick vacuum suction, dissolved in the NMR solvent, and pressed with nitrogen through a pipet filled with filter flakes into the NMR tube. To ensure representative samples, all of the material must dissolve completely in the NMR solvent; any residual product was flushed into the NMR tube in the same way. The relative de was determined by the integrals of the particular ³¹P and ¹H NMR signals.

Mp: 199 °C (dec). [α]_D²³ –111.5 (CH₂Cl₂, *c* 0.0029). ¹H NMR (500 MHz, acetone-*d*₆; **7S**): 7.86–7.80 (m, 4H, 2,6-H of –PPh₂); 7.64–7.50 (m, 6H, 3,4,5-H of –PPh₂); 7.37–7.33 (m, 4H, 2,3,5,6-H of PhNH₂); 7.24–7.20 (m, 1H, 4-H of PhNH₂); 6.56 (pseudo t, 1H, 4-H of *η*⁶-Ph); 6.09 (pseudo t, 1H, 5-H of *η*⁶-Ph); 5.75 (m, 1H, 2-H of *η*⁶-Ph); 5.60 (not res. d, 1H, –NH₂); 5.51 (m, 1H, 6-H of *η*⁶-Ph); 5.48 (m, 1H, 3-H of *η*⁶-Ph); 4.91 (not res. d, 1H, –NH₂); 4.62 (not res. ddd, 1H, –CH₂–); 4.57 (not res. ddd, 1H, –CH–); 4.44 (ddd, ²*J*_{H,H} = 17.0, ³*J*_{H,H} = 12.5, ³*J*_{H,P} = 2.5, 1H, –CH₂–); 3.56 (s, 3H, –CH₃). ¹³C{¹H} NMR (126 MHz, acetone-*d*₆; **7S**): δ 148.54 (1-C of PhNH₂); 134.45 (d, ²*J*_{C,P} = 13.4, 2,6-C of –PPh₂); 133.21 (d, ⁴*J*_{C,P} = 62.1, 4-C of –PPh₂); 131.65 (d, ²*J*_{C,P} = 10.3, 2,6-C of –PPh₂); 130.24 (d, ³*J*_{C,P} = 11.4, 3,5-C of –PPh₂); 130.16 (3,5-C of PhNH₂); 129.52 (d, ³*J*_{C,P} = 11.3, 3,5-C of –PPh₂); 126.84 (4-C of PhNH₂); 121.75 (2,6-C of PhNH₂); 107.56 (6-C of *η*⁶-Ph); 103.10 (d, ²*J*_{C,P} = 10.3, 4-C of *η*⁶-Ph); 95.85 (1-C of *η*⁶-Ph); 86.97 (5-C of *η*⁶-Ph); 82.54 (3-C of *η*⁶-Ph); 81.71 (2-C of *η*⁶-Ph); 73.23 (–CH–); 68.19 (–CH₂–); 58.24 (–CH₃). ³¹P{¹H} NMR (121 MHz, acetone-*d*₆; **7S**): δ 131.75 (s, 1P). FAB⁺-MS; *m/z* (%): 436 (59) [M – Cl – C₆H₇N – PF₆]⁺ with respect to ¹⁰²Ru, 472 (100) [M – C₆H₇N – PF₆]⁺ with respect to ¹⁰²Ru, 565 (43) [M – PF₆]⁺ with respect to ¹⁰²Ru. C₂₇H₂₈ClF₆NO₂P₂Ru (710.99): calcd C 45.61, H 3.97, N 1.97; found C 45.35, H 4.03, N 1.83.

(*1R*)-[*σ*-Chloro-*σ*(*N*)-(4-fluorophenylamino)-{*σ*(*P*):*η*⁶-(2-(*P,P*-diphenylphosphinoxy)-1'-methoxyethyl)benzene}]ruthenium(II)] Hexafluorophosphate (**8**). **8** was prepared according to the procedure above from 392 mg (0.771 mmol) of **6**, 035 mL (405 mg, 3.644 mmol) of *p*-fluoroaniline, and 406 mg (2.417 mmol) of NaPF₆

in 4.5 mL of CH₂Cl₂ and 9 mL of MeOH. Before workup 66% de (**8S**) was determined by NMR. After workup 686 mg of crude **8** were obtained as a brownish microcrystalline powder. The crude product was recrystallized from MeOH (reflux/–30 °C) to give finally 293 mg (0.393 mmol, 51%) of pure **8** with **8S**:**8R** = 1:1 (NMR, X-ray crystal structure analysis). **8** is also soluble in CH₂Cl₂, CHCl₃, and acetone. Mp: 188–190 °C (dec). [α]_D²³ –34.9 (CH₂Cl₂, *c* 0.0038).

Properties of epimeric mixtures **8S**/**8R** = 1:1: ¹H NMR (500 MHz, acetone-*d*₆; signals that are assigned to a specific diastereomer are characterized by *R* or *S*): δ 7.90–7.75 and 7.63–7.50 (m, 20H, –PPh₂); 7.40 (m, 4H, 2,6-H of (*p*-F)C₆H₄NH₂); 7.10 (pseudo t, 4H, 3,5-H of (*p*-F)C₆H₄NH₂); 6.59 (pseudo t, 1H, 4-H of *η*⁶-Ph, *S*); 6.56 (pseudo t, 1H, 4-H of *η*⁶-Ph, *R*); 6.11 (pseudo t, 1H, 3-H of *η*⁶-Ph, *S*); 6.08 (pseudo t, 1H, 3- or 5-H of *η*⁶-Ph, *R*); 6.01 (br s, 2H, –NH₂); 5.87 (pseudo t, 1H, 2- or 6-H of *η*⁶-Ph, *R*); 6.77 (pseudo d, 1H, 6- or 2-H of *η*⁶-Ph, *R*); 5.75 (pseudo t, 1H, 2-H of *η*⁶-Ph, *S*); 5.65 (m, 1H, 5-H of *η*⁶-Ph, *S*); 5.63 (pseudo t, 1H, 6-H of *η*⁶-Ph, *S*); 5.38 (m, 1H, 5- or 3-H of *η*⁶-Ph, *R*); 4.95 (not res. br d, 2H, –NH₂); 4.69 (m, 2H, –CH₂–, *S* and *R*); 4.56 (m, 1H, –CH–, *S*); 4.54 (m, 1H, –CH–, *R*); 4.52–4.42 (m, 2H, –CH₂–, *S* and *R*); 3.56 (s, 3H, –CH₃, *S*); 3.42 (s, 3H, –CH₃, *R*). ¹³C{¹H} NMR (126 MHz, acetone-*d*₆): δ 161.13 (d, ¹*J*_{C,F} = 127.2, 4-C of (*p*-F)C₆H₄NH₂, *S* and *R*); 145.03 (d, ¹*J*_{C,F} = 100.3, 1-C of (*p*-F)C₆H₄NH₂, *S* and *R*); 136.42 (d, ¹*J*_{C,P} = 63.1, 1-C of –PPh₂); 135.67 (d, ¹*J*_{C,P} = 63.1, 1-C of –PPh₂); 134.50–129.36 (series of d, –PPh₂); 123.79 (d, ³*J*_{C,F} = 8.3, 2,6-C of (*p*-F)C₆H₄NH₂, *S* or *R*); 123.39 (d, ³*J*_{C,F} = 8.3, 2,6-C of (*p*-F)C₆H₄NH₂, *R* or *S*); 116.86 (d, ²*J*_{C,F} = 19.6, 3,5-C of (*p*-F)C₆H₄NH₂, *S* or *R*); 116.68 (d, ³*J*_{C,F} = 18.6, 3,5-C of (*p*-F)C₆H₄NH₂, *R* or *S*); 108.32 (5- or 3-C of *η*⁶-Ph, *R*); 107.41 (5-C of *η*⁶-Ph, *S*); 102.98 (4-C of *η*⁶-Ph, *S* and *R*); 96.05 (1-C of *η*⁶-Ph, *S*); 94.73 (1-C of *η*⁶-Ph, *R*); 87.63 (3- or 5-C of *η*⁶-Ph, *R*); 87.17 (3-C of *η*⁶-Ph, *S*); 83.68 (d, ²*J*_{C,P} = 7.3, 6- or 2-C of *η*⁶-Ph, *R*); 82.44 (2- or 6-C of *η*⁶-Ph, *R*; 6-C of *η*⁶-Ph, *S*); 81.78 (2-C of *η*⁶-Ph, *S*); 75.18 (–CH–, *R*); 73.25 (–CH–, *S*); 70.31 (–CH₂–, *S* and *R*); 58.19 (d, ²*J*_{C,P} = 6.2, –CH₃, *S*); 57.75 (–CH₃, *R*). ³¹P{¹H} NMR (109 MHz, CDCl₃): δ 133.29 (s, 1P, *S*); 129.83 (s, 1P, *R*). FAB⁺-MS; *m/z* (%) 438 (94) [M – Cl – C₆H₆FN – PF₆]⁺ with respect to ¹⁰²Ru, 472 (100) [M – C₆H₆FN – PF₆]⁺ with respect to ¹⁰²Ru, 585 (28) [M – PF₆]⁺ with respect to ¹⁰²Ru. C₂₇H₂₇ClF₇NO₂P₂Ru(MeOH)_{0.5} (745.00): calcd C 44.34, H 3.92, N 1.88; found C 44.31, H 3.65, N 1.91.

(*R*_{Ru},*1R*,*1R*)-[*σ*-Chloro{*σ*(*P*):*η*⁶-[(2-(*P,P*-diphenylphosphinoxy)-1-methoxyethyl)benzene]}-*σ*(*N*)-(1'-phenylethylamino)ruthenium(II)] Hexafluorophosphate (**9R**). **9** was prepared according to the procedure above from 389 mg (0.765 mmol) of **6**, 0.27 mL (257 mg, 2.117 mmol) of (*R*)-1-phenylethylamine, and 440 mg (2.620 mmol) of NaPF₆ in 3 mL of CH₂Cl₂ and 9 mL of MeOH. No de was detectable by NMR before workup. After workup 699 mg of crude **9** was obtained as a yellow solid foam with 7% de (**9R**) [³¹P{¹H} NMR (109 MHz, acetone-*d*₆; **9S**): δ 135.29 (s, 1P); ¹H NMR (270 MHz, acetone-*d*₆; **9S**): δ 3.49 (s, 3H, –CH₃)]. The crude product was recrystallized from a small amount of MeOH at –30 °C to yield 151 mg (0.204 mmol, 27%) of pure **9R** with >99% de by NMR. The crystals were suitable for X-ray structure determination. The compound is also soluble in CH₂Cl₂, CHCl₃, and acetone. Mp: 169 °C. [α]_D²³ +38.4 (CH₂Cl₂, *c* 0.0037). ¹H NMR (400 MHz, acetone-*d*₆; **9R**): δ 7.88–7.82 and 7.75–7.70 and 7.61–7.47 (3 m, 10H, –PPh₂); 7.34–7.27 (m, 3H, 3,4,5-H of PhCH(CH₃)NH₂); 7.10–7.06 (m, 2H, 2,6-H of PhCH(CH₃)NH₂); 6.79 (pseudo t, 1H, 4-H of *η*⁶-Ph); 6.68 (pseudo t, 1H, 3- or 5-H of *η*⁶-Ph); 6.22 (pseudo t, 1H, 2- or 6-H of *η*⁶-Ph); 6.01 (pseudo t, 1H, 6- or 2-H of *η*⁶-Ph); 5.20 (pseudo d, 1H, 5- or 3-H of *η*⁶-Ph); 4.40 (m, 1H, –CH(OCH₃)–); 4.35 (2 m, 2H, –CH₂–); 3.80 (q, ³*J*_{H,H} = 6.5; 1H, –CH(CH₃)NH₂); 3.65 (br s, 2H, –NH₂); 3.36 (s, 3H, –OCH₃); 1.23 (d, ³*J*_{H,H} = 6.5, 3H, –CH(CH₃)NH₂). ¹³C{¹H} NMR (68 MHz, acetone-*d*₆; **9R**): δ 143.90 (1-C of

PhCH(CH₃)NH₂); 135.82 (d, ¹J_{C,P} = 59.9, 1-C of -PPh₂); 134.28 (d, ²J_{C,P} = 12.3, 2,6-C of -PPh₂); 133.20 (d, ⁴J_{C,P} = 2.5, 4-C of -PPh₂); 132.86 (d, ⁴J_{C,P} = 2.8, 4-C of -PPh₂); 132.09 (d, ¹J_{C,P} = 52.1, 1-C of -PPh₂); 131.23 (d, ²J_{C,P} = 10.3, 2,6-C of -PPh₂); 130.26 (d, ³J_{C,P} = 10.6, 3,5-C of -PPh₂); 129.69 (3,5-C of *PhCH(CH₃)NH₂*); 129.28 (d, ³J_{C,P} = 11.4, 3,5-C of -PPh₂); 129.00 (4-C of *PhCH(CH₃)NH₂*); 126.99 (2,6-C of *PhCH(CH₃)NH₂*); 103.25 (d, ²J_{C,P} = 7.5, 4-C of η^6 -Ph); 101.89 (d, ²J_{C,P} = 10.6, 3- or 5-C of η^6 -Ph); 93.82 (1-C of η^6 -Ph); 90.97 (2- or 6-C of η^6 -Ph); 82.94 (6- or 2-C of η^6 -Ph); 82.19 (5- or 3-C of η^6 -Ph); 75.28 (-CH₂-); 68.87 (-CH(OCH₃)-); 58.13 (-CH(CH₃)NH₂); 57.66 (-OCH₃); 23.81 (-CH(CH₃)NH₂). ³¹P{¹H} NMR (109 MHz, acetone-*d*₆; **9R**): δ 133.19 (s, 1P). FAB⁺-MS: *m/z* (%) 436 (76) [M - Cl - C₈H₁₃N - PF₆⁻]⁺ with respect to ¹⁰²Ru, 472 (100) [M - C₈H₁₃N - PF₆⁻]⁺ with respect to ¹⁰²Ru, 593 (43) [M - PF₆⁻]⁺ with respect to ¹⁰²Ru. C₂₉H₃₂ClF₆NO₂P₂Ru (739.04): calcd C 47.13, H 4.36, N 1.90; found C 47.06, H 4.39, N 1.93.

(1R,1'S)-[σ -Chloro- $\{\sigma(P):\eta^6$ -(2-(*P,P*-diphenylphosphinoxy)-1-methoxyethyl)benzene]- $\sigma(N)$ -(1'-phenylethylamino)ruthenium(II) hexafluorophosphate (10). **10** was prepared according to the procedure above from 392 mg (0.771 mmol) of **6**, 0.23 mL (219 mg, 1.803 mmol) of (*S*)-1-phenylethylamine, and 432 mg (2.572 mmol) of NaPF₆ in 3 mL of CH₂Cl₂ and 9 mL of MeOH. No de was detectable by NMR before and after workup. After workup 665 mg of crude **10** was obtained as a brownish solid foam. The crude product was precipitated from MeOH at -30 °C to give 84 mg (0.204 mmol, 27%) of **10** as a brown powder with (**10S**): (**10R**) = 1:1 by NMR. In one batch eventually one crystal could be found in the product (which was not crystalline otherwise) suitable for X-ray crystal structure analysis, which contained **10S** only. The compound is also soluble in CH₂Cl₂, CHCl₃, and acetone. Mp: 156–157 °C. [α]_D²³ -49.1 (CH₂Cl₂, *c* 0.0018).

Properties of epimeric mixtures **10S/10R** = 1:1: ¹H NMR (400 MHz, acetone-*d*₆): δ 7.89–7.80 and 7.67–7.49 (2 m, 20H, -PPh₂); 7.36–7.21 (m, 6H, 3,4,5-H of *PhCH(CH₃)NH₂*); 7.09–7.05 (m, 4H, 2,6-H of *PhCH(CH₃)NH₂*); 6.74 (pseudo t, 1H, 5-H of η^6 -Ph, *S*); 6.61 (pseudo q, 2H, 4-H of η^6 -Ph, *S* and *R*); 6.21 (pseudo t, 1H, 3-H of η^6 -Ph, *S*); 6.17 (pseudo t, 1H, 3- or 5-H of η^6 -Ph, *R*); 6.03 (pseudo t, 1H, 2- or 6-H of η^6 -Ph, *R*); 6.00 (pseudo t, 1H, 5- or 3-H of η^6 -Ph, *R*); 5.87 (m, 1H, 2-H of η^6 -Ph, *S*); 5.64 (pseudo d, 1H, 6- or 2-H of η^6 -Ph, *R*); 5.33 (pseudo d, 1H, 6-H of η^6 -Ph, *S*); 4.77 (ddd, ²J_{H,H} = 23.3, ³J_{H,H} = 13.0, ³J_{H,P} = 4.0, 1H, -CH₂-, *S*); 4.54 (m, 1H, -CH(OCH₃)-, *S*); 4.46 (not res. ddd, 1H, -CH₂-, *R*); 4.32 (m, 1H, -CH(OCH₃)-, *R*); 4.30 (not res. q, 1H, -CH(CH₃)NH₂, *R*); 4.26 (m, 1H, -CH₂-, *R*); 4.20 (not res. ddd, 1H, -CH₂-, *S*); 3.82 (q, ³J_{H,H} = 6.5, 1H, -CH(CH₃)NH₂, *S*); 3.59 (s, 3H, -OCH₃, *S*); 3.36 (s, 3H, -OCH₃, *R*); 1.30 (d, ³J_{H,H} = 6.5, 3H, -CH(CH₃)NH₂, *R*); 1.05 (d, ³J_{H,H} = 6.5, 3H, -CH(CH₃)NH₂, *S*). ¹³C{¹H} NMR (126 MHz, acetone-*d*₆): δ 144.19 (1-C of *PhCH(CH₃)NH₂*, *R*); 143.96 (1-C of *PhCH(CH₃)NH₂*, *S*); 135.83–129.12 (series of d, -PPh₂); 133.06 (4-C of *PhCH(CH₃)NH₂*, *S* and *R*); 129.86 (3,5-C of *PhCH(CH₃)NH₂*, *S* or *R*); 129.73 (3,5-C of *PhCH(CH₃)NH₂*, *R* or *S*); 127.12 (2,6-C of *PhCH(CH₃)NH₂*, *R* or *S*); 103.58 (5-C of η^6 -Ph, *S*; or 5- or 3-C of η^6 -Ph, *R*); 103.53 (5- or 3-C of η^6 -Ph, *R*; or 5-C of η^6 -Ph, *S*); 102.11 (d, ²J_{C,P} = 10.3, 4-C of η^6 -Ph, *R*); 101.70 (d, ²J_{C,P} = 10.3, 4-C of η^6 -Ph, *S*); 95.00 (1-C of η^6 -Ph, *S*); 93.97 (1-C of η^6 -Ph, *R*); 89.97 (3-C of η^6 -Ph, *S*); 89.72 (3- or 5-C of η^6 -Ph, *R*); 83.23 (2- or 6-C of η^6 -Ph, *R*); 82.35 (6- or 2-C of η^6 -Ph, *R*); 81.62 (2-C of η^6 -Ph, *S*); 79.85 (6-C of η^6 -Ph, *S*); 75.15 (-CH(OCH₃)-, *R*); 72.58 (-CH(OCH₃)-, *S*);

69.63 (-CH₂-, *R*); 66.65 (-CH₂-, *S*); 59.22 (-CH(CH₃)NH₂, *S*); 58.83 (-CH(CH₃)NH₂, *R*); 58.20 (-OCH₃, *S*); 57.69 (-OCH₃, *R*); 24.68 (-CH(CH₃)NH₂, *R*); 24.26 (-CH(CH₃)NH₂, *S*). ³¹P{¹H} NMR (109 MHz, acetone-*d*₆): δ 133.77 (s, 1P); 129.16 (s, 1P). FAB⁺-MS: *m/z* (%) 438 (88) [M - Cl - C₈H₁₃N - PF₆⁻]⁺ with respect to ¹⁰²Ru, 474 (100) [M - C₈H₁₃N - PF₆⁻]⁺ with respect to ¹⁰²Ru, 595 (39) [M - PF₆⁻]⁺ with respect to ¹⁰²Ru. C₂₉H₃₂ClF₆NO₂P₂Ru (739.04): calcd C 47.13, H 4.36, N 1.90; found C 47.48, H 4.29, N 2.01.

Crystal Structure Determination. Details of crystal parameters, data collection, and structure refinement are summarized in Table 8. X-ray diffraction data were collected at 100 K on a Bruker-Nonius KappaCCD diffractometer (Mo K α radiation, λ = 0.71073 Å, graphite monochromator). Data were corrected for Lorentz and polarization effects. Absorption correction was performed by numerical Gauss integration^{17a} or on the basis of multiple scans with SADABS.^{17b} All structures were solved by direct methods and refined by full-matrix least-squares procedures on *F*² in the anisotropic approximation for all atoms except hydrogen.^{17c} The absolute configurations were confirmed respectively by anomalous dispersion effects (*f'* and *f''*)^{18a} and the calculation of Flack's absolute structure parameter.^{18b} All hydrogen atoms are in positions calculated for optimized geometry and are assigned an isotropic displacement parameter equivalent to the 1.2-fold and 1.5-fold value of the equivalent isotropic displacement parameter of their carrier atoms. In the crystal structure of **9R**·(MeOH) phenyl ring C31–C36 is disordered; two alternative orientations have been refined that are occupied by 69.9(7)% for C31–C36 and 30.1(7)% for C31A–C36A, respectively. CCDC-665181 (for **6**), CCDC-665182 (for **7R**), CCDC-665183 (for **8**·(MeOH)_{0.5}), CCDC-665184 (for **9R**·(MeOH)), and CCDC-665185 (for **10S**) contain the supplementary crystallographic data for this paper. These data can be obtained free of charge via http://www.ccdc.cam.ac.uk/data_request/cif (or from Cambridge Crystallographic Data Centre, 12 Union Road, Cambridge, CB2 1EZ, UK (fax: ++44-1223-336-033; e-mail: deposit@ccdc.cam.ac.uk).

Acknowledgment. We are grateful to the Deutsche Forschungsgemeinschaft (SFB 583 and GRK 312) for financial support, Prof. Dr. Tim Clark (CCC and ICMM FAU Erlangen-Nürnberg) for hosting one of us (I.W.) in 2003, Prof. Dr. Peter Gmeiner (Dept. Chemie and Pharmazie, Emil Fischer Zentrum, FAU) and Prof. Dr. Andreas Hirsch for providing access to essential analytical equipment, Dr. Matthias Moll for recording 1D and 2D NMR spectra of complex **9R**, and Prof. Dr. Rudi van Eldik and Dr. Ralf Puchta for many fruitful discussions (all Department Chemie and Pharmazie and ICMM FAU Erlangen-Nürnberg).

Supporting Information Available: Crystallographic information files (CIF) of all X-ray structure investigations of this paper. NMR and catalytic transfer hydrogenation study (3 figures, 1 table). The assignments of the ¹H NMR and ¹³C NMR signals belonging to the particular diastereomers of mixtures **8S/8R** and **10S/10R** on the basis of diastereomerically pure **7S** by detailed NOE measurements. This material is available free of charge via the Internet at <http://pubs.acs.org> or from the authors.

OM701257M